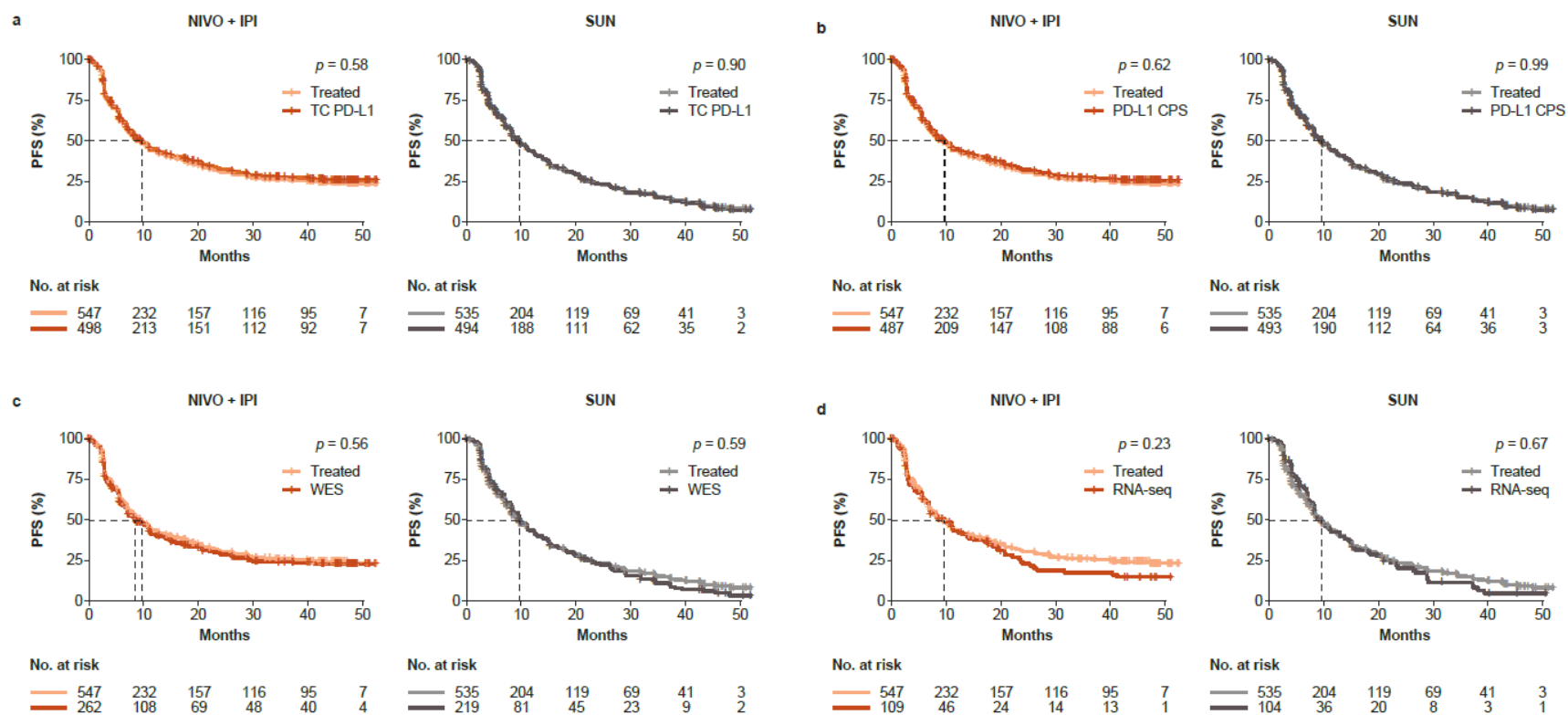
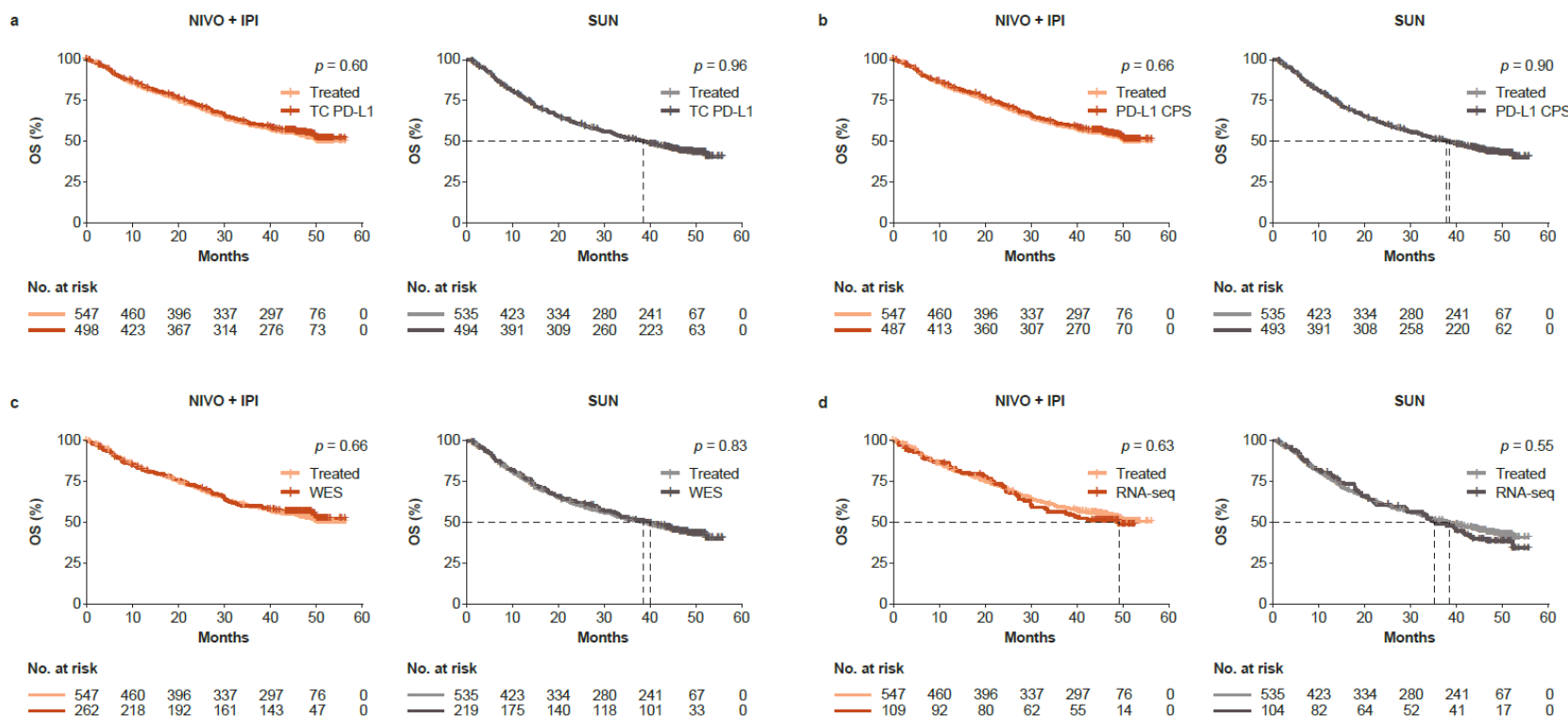


Supplementary Figure 1. PFS versus biomarker availability by treatment arm in CheckMate 214. CPS, combined positive score; IPI, ipilimumab; NIVO, nivolumab; PD-L1, programmed death ligand 1; PFS, progression-free survival; RNA-seq, RNA sequencing; SUN, sunitinib; TC, tumor cell; WES, whole-exome sequencing.

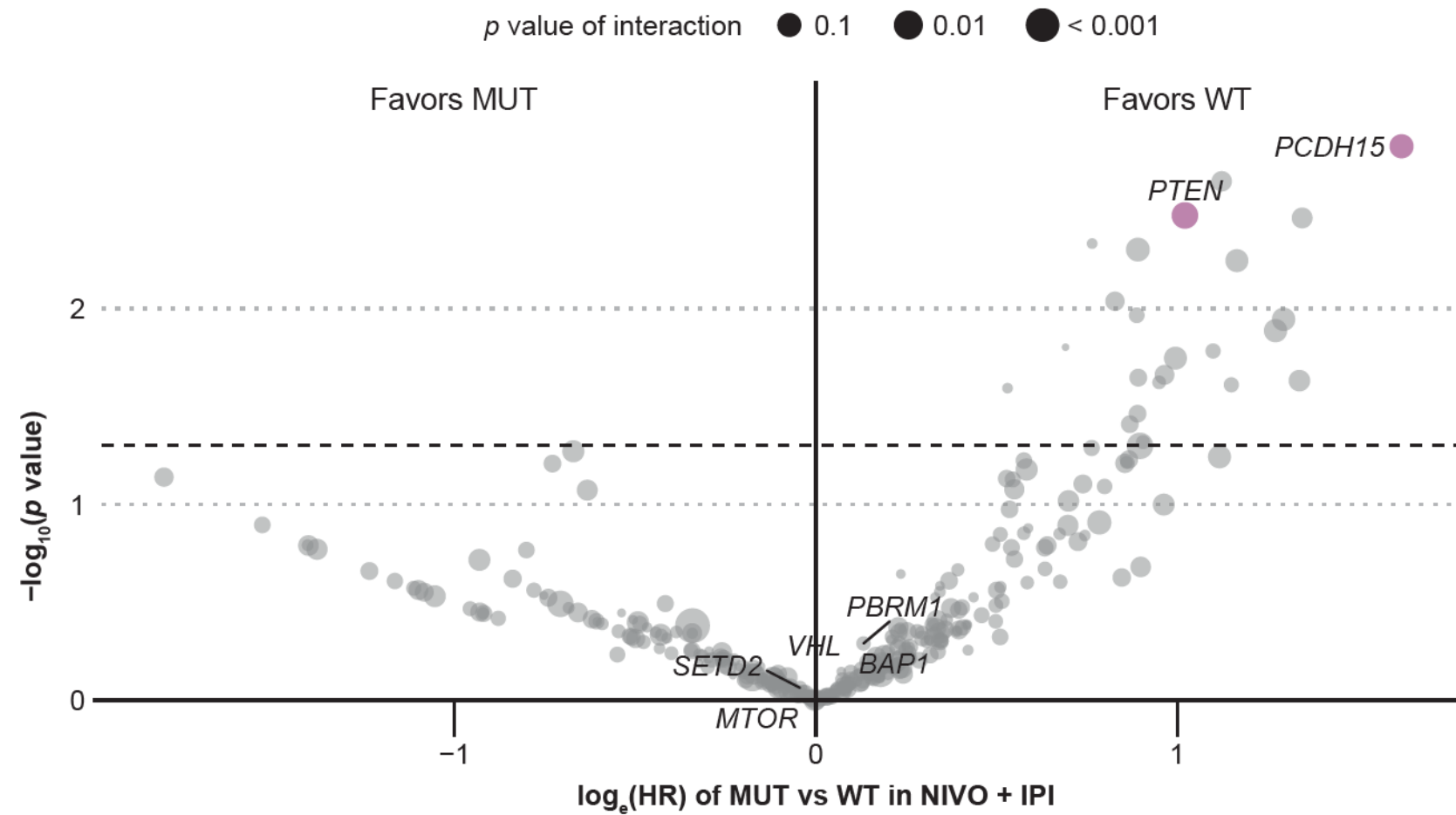


Supplementary Figure 2. OS versus biomarker availability by treatment arm in CheckMate 214. CPS, combined positive score;

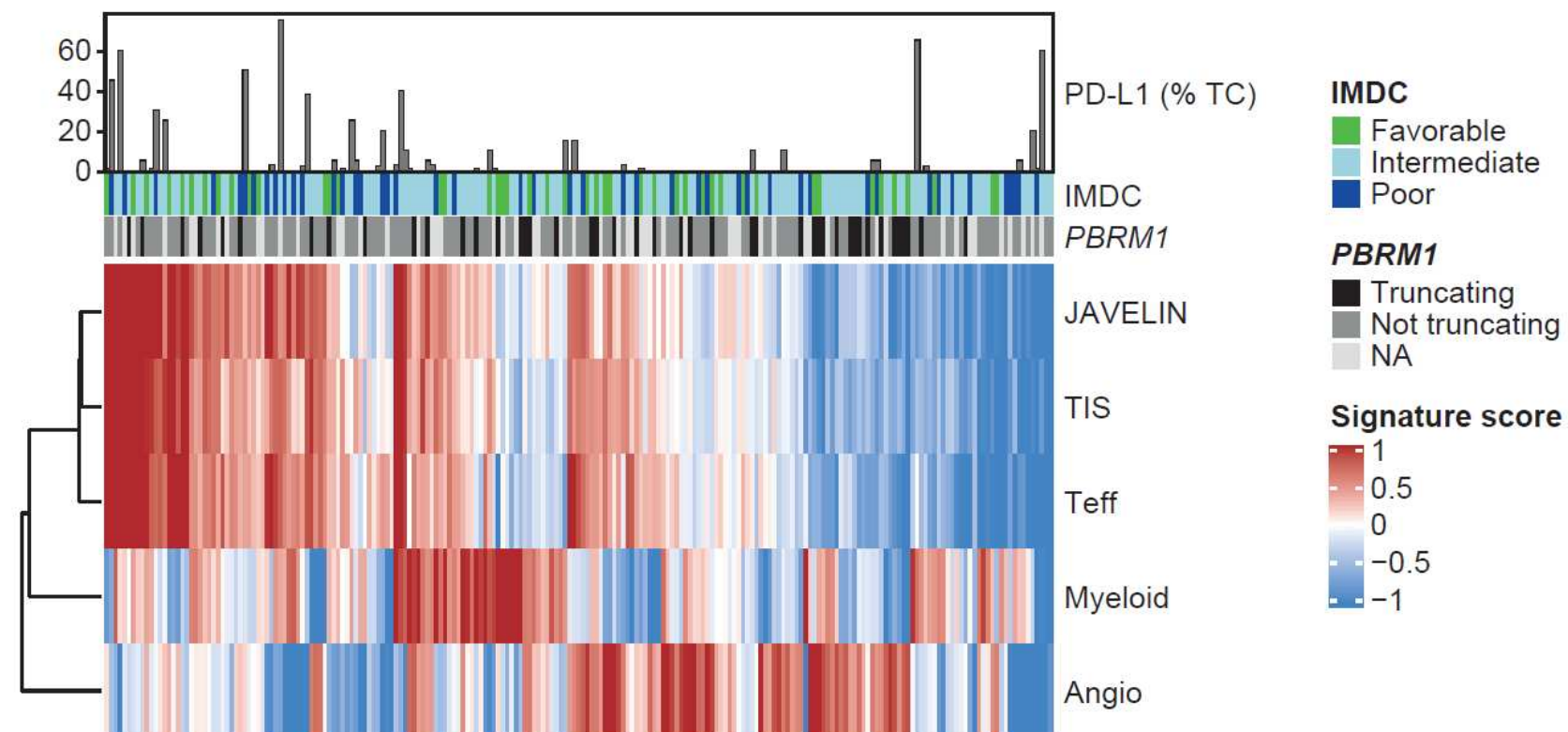
IPI, ipilimumab; NIVO, nivolumab; OS, overall survival; PD-L1, programmed death ligand 1; RNA-seq, RNA sequencing; SUN, sunitinib; TC, tumor cell; WES, whole-exome sequencing.



Supplementary Figure 3. Volcano plot of the association of mutation status with OS with NIVO plus IPI for the 382 genes that were mutated in ≥ 10 of the 481 WES-evaluable patients from CheckMate 214 (prevalence >2%). The y-axis represents $-\log_{10}$ of the p value for association of mutation status with OS with NIVO plus IPI; the horizontal black dashed line indicates $p=0.05$. The x-axis represents $\log_e(\text{HR})$ for OS in patients with MUT versus WT status. Sizes of circles on the graph indicate p value of the interaction between the treatment arm and the gene mutation. The genes highlighted in pink showed association with OS with NIVO plus IPI ($p<0.05$) and an interaction between mutation status and treatment arm ($p<0.05$). However, no associations reached statistical significance for any gene after adjustment for multiple hypothesis testing. The frequency of mutations found in the labeled genes is provided in Figure 2C. HR, hazard ratio; IPI, ipilimumab; MUT, mutant; NIVO, nivolumab; OS, overall survival; WES, whole-exome sequencing; WT, wild-type.

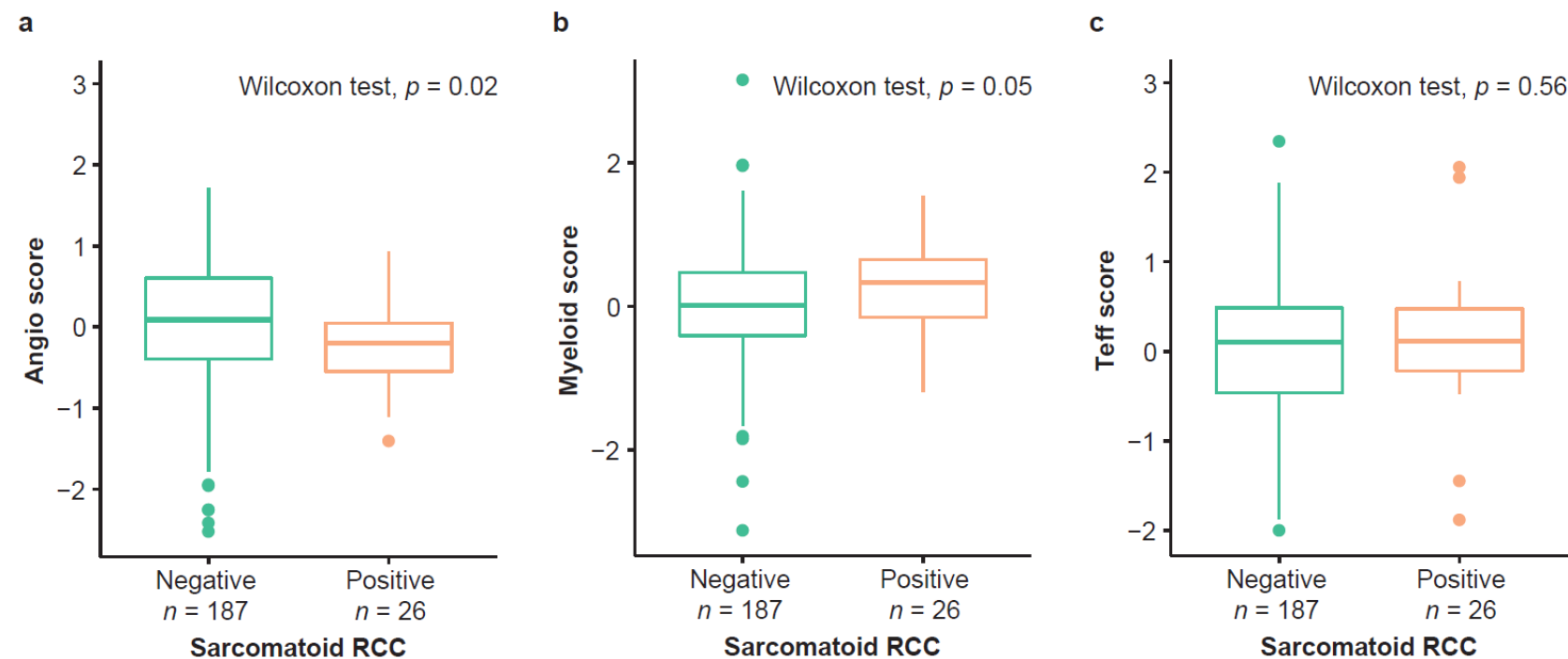


Supplementary Figure 4. Heatmap showing relationship between gene expression signatures, PD-L1 expression levels, *PBRM1* mutation status, and IMDC status. Angio, IMmotion 150 Angiogenesis gene expression signature; IMDC, International Metastatic RCC Database Consortium; JAVELIN, JAVELIN Renal 101 gene expression signature; Myeloid, IMmotion150 gene expression signature; NA, not available; PD-L1, programmed death ligand 1; TC, tumor cell; Teff, IMmotion150 T-effector gene expression signature; TIS, Tumor Inflammation Signature.

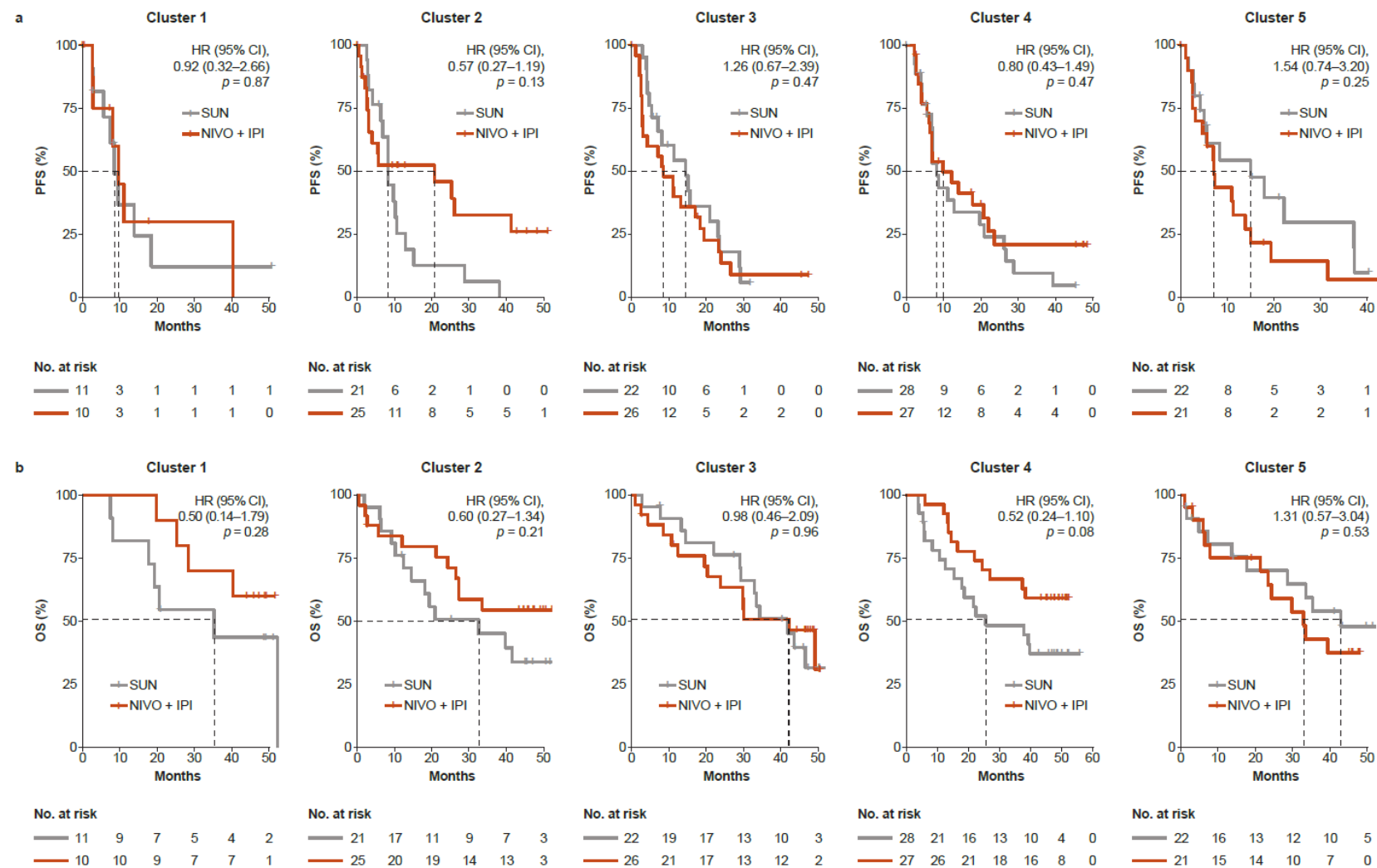


Supplementary Figure 5. Relationship of gene expression signature scores with sarcomatoid histology. Angio, IMmotion 150

Angiogenesis gene expression signature; Myeloid, IMmotion150 gene expression signature; RCC, renal cell carcinoma; Teff, IMmotion150 T-effector gene expression signature.



Supplementary Figure 6. Survival by MCP-counter cluster and treatment arm. (A) PFS by MCP-counter cluster and treatment arm. (B) OS by MCP-counter cluster and treatment arm (HRs and 95% CIs reflect comparisons between patients in the NIVO plus IPI versus SUN arms. P value computed based on log-rank test comparing PFS or OS among the five clusters within each treatment arm). After adjusting for multiplicity, no association reached statistical significance. CI, confidence interval; HR, hazard ratio; IPI, ipilimumab; MCP, Microenvironment Cell Population; NIVO, nivolumab; OS, overall survival; PFS, progression-free survival; SUN, sunitinib.



Supplementary Table 1 Treated biomarker-evaluable patient populations for exploratory analyses.

	NIVO + IPI (n=550)	SUN (n=546)
Biomarkers evaluated	Evaluable samples, n	
PD-L1 IHC^a		
Tumor cell (TC PD-L1)	498	494
Combined positive score (PD-L1 CPS)	487	493
WES	262	219
RNA-seq	109	104

^aPD-L1 IHC performed using the Dako PD-L1 IHC 28-8 pharmDx assay. CPS, combined positive score; IHC, immunohistochemistry; IPI, ipilimumab; NIVO, nivolumab; PD-L1, programmed death ligand 1; RNA-seq, RNA sequencing; SUN, sunitinib; TC, tumor cell; WES, whole-exome sequencing.

Supplementary Table 2 Dispositions and baseline characteristics of patient population.

	ITT (n=1096)	Treated (n=1082)	TC PD-L1 (n=992)	PD-L1 CPS (n=980)	WES (n=481)	RNA-seq (n=213)
Randomized to NIVO+IPI, n	550	547	498	487	262	109
Randomized to SUN, n	546	535	494	493	219	104
Sex (%)						
Male	808 (73.7)	797 (73.7)	726 (73.2)	717 (73.2)	348 (72.3)	155 (72.8)
Age						
Mean (SD)	60.8 (9.94)	60.9 (9.91)	60.9 (9.90)	61.0 (9.80)	60.8 (9.90)	62.0 (9.56)
Median	62.0	62.0	62.0		61.0	63.0
(min–max)	(21.0–85.0)	(21.0–85.0)	(21.0–85.0)		(25.0–85.0)	(31.0–85.0)

Missing (%)	28 (2.6)	28 (2.6)	25 (2.5)	62.0 (21.0–85.0)	12 (2.5)	5 (2.3)
IMDC (%)				25 (2.6)		
Poor	198 (18.1)	195 (18.0)	175 (17.6)	172 (17.6)	87 (18.1)	46 (21.6)
Intermediate	665 (60.7)	660 (61.0)	612 (61.7)	604 (61.6)	297 (61.7)	122 (57.3)
Favorable	232 (21.2)	226 (20.9)	204 (20.6)	203 (20.7)	96 (20.0)	45 (21.1)
Not reported	1 (0.1)	1 (0.1)	1 (0.1)	1 (0.1)	1 (0.2)	0 (0)
Tumor location (%)						
Primary site	874 (79.7)	863 (79.8)	804 (81.0)	792 (80.8)	403 (83.8)	151 (70.9)
Metastatic site	206 (18.8)	203 (18.8)	182 (18.3)	174 (17.8)	75 (15.6)	61 (28.6)
No tissue available	9 (0.8)	9 (0.8)	0 (0.0)	8 (0.8)	0 (0.0)	0 (0.0)

Not reported	7 (0.6)	7 (0.6)	6 (0.6)	6 (0.6)	3 (0.6)	1 (0.5)
--------------	---------	---------	---------	---------	---------	---------

CPS, combined positive score; IMDC, International Metastatic RCC Database Consortium; IPI, ipilimumab; ITT, intent-to-treat; NIVO, nivolumab; PD-L1, programmed death ligand 1; RNA-seq, RNA sequencing; SD, standard deviation; SUN, sunitinib; TC, tumor cell; WES, whole-exome sequencing.

Supplementary Table 3 Statistical analyses for associations with PD-L1 expression^a.

Cutoff	Arm used for comparison	PFS		OS	
		Nominal p	Adjusted p	Nominal p	Adjusted p
≥1% TC	NIVO+IPI (n=113) vs SUN (n=125)	<0.0001	<0.0001	<0.01	<0.01
<1% TC	NIVO+IPI (n=385) vs SUN (n=369)	0.37	0.56	0.02	0.03
CPS ≥1	NIVO+IPI (n=298) vs SUN (n=298)	<0.0001	<0.0001	<0.01	<0.01
CPS <1	NIVO+IPI (n=189) vs SUN (n=195)	0.76	0.91	0.03	0.03
≥1% TC vs <1% TC (n=113 ≥1% vs 385 <1%)	NIVO+IPI	0.02	0.04	0.96	0.96
CPS ≥1 vs CPS <1 (n=298 ≥1 vs 189 <1)	NIVO+IPI	0.95	0.95	0.02	0.03

^aNominal and adjusted p values are shown to accompany figure 1. Adjusted p values were corrected for multiple hypothesis testing using the Benjamini–Hochberg procedure. CPS, combined positive score; IPI, ipilimumab; NIVO, nivolumab; OS, overall survival; PD-L1, programmed death ligand 1; PFS, progression-free survival; SUN, sunitinib; TC, tumor cell.

Supplementary Table 4 Statistical analyses for associations with genomic biomarkers^a.

Biomarker	Cutoff	Arm used for comparison	PFS		OS	
			Nominal p	Adjusted p	Nominal p	Adjusted p
TMB	≥ median vs < median	NIVO+IPI	0.76	0.76	0.10	0.14
		SUN	0.40	0.60	0.96	0.96
TIB	≥ median vs < median	NIVO+IPI	0.38	0.57	0.12	0.14
		SUN	<0.01	0.01	0.05	0.16
HLA status	Heterozygous vs homozygous	NIVO+IPI	0.10	0.31	0.14	0.14
		SUN	0.71	0.71	0.15	0.22

^aNominal and adjusted p values are shown to accompany figures 2A and 2B. Adjusted p values were corrected for multiple hypothesis testing using the Benjamini–Hochberg procedure. HLA, human leukocyte antigen; IPI, ipilimumab; NIVO, nivolumab; OS, overall survival; PFS, progression-free survival; SUN, sunitinib; TIB, tumor indel burden; TMB, tumor mutational burden.

Supplementary Table 5 Statistical analyses for associations with gene mutation status^a.

Gene	Cutoff	Arm used for comparison	PFS		OS	
			Nominal p	Adjusted p	Nominal p	Adjusted p
<i>VHL</i>	MUT vs WT	NIVO+IPI	0.52	0.63	0.71	0.97
		SUN	0.47	0.63	0.64	0.97
<i>PBRM1</i>	MUT vs WT	NIVO+IPI	0.04	0.35	0.51	0.97
		SUN	0.18	0.61	0.92	0.97
<i>SETD2</i>	MUT vs WT	NIVO+IPI	0.57	0.63	0.86	0.97
		SUN	0.09	0.43	0.38	0.97
<i>BAP1</i>	MUT vs WT	NIVO+IPI	0.70	0.70	0.78	0.97
		SUN	0.37	0.63	0.35	0.97
<i>MTOR</i>	MUT vs WT	NIVO+IPI	0.54	0.63	0.97	0.97
		SUN	0.52	0.63	0.29	0.97

^aNominal and adjusted p values are shown to accompany figures 2C, 2D, and 2E. Adjusted p values were corrected for multiple hypothesis testing using the Benjamini–Hochberg procedure. IPI, ipilimumab; MUT, mutant; NIVO, nivolumab; OS, overall survival; PFS, progression-free survival; SUN, sunitinib; WT, wild-type.

Supplementary Table 6 Statistical analyses for associations with gene expression signature score^a.

Gene expression signature	Cutoff	Arm used for comparison	PFS		OS	
			Nominal p	Adjusted p	Nominal p	Adjusted p
Angio	≥ median vs < median	NIVO+IPI	0.35	0.82	0.71	0.93
		SUN	0.02	0.15	0.16	0.81
JAVELIN	≥ median vs < median	NIVO+IPI	0.83	0.83	0.32	0.93
		SUN	0.98	0.98	0.62	0.81
TIS	≥ median vs < median	NIVO+IPI	0.57	0.83	0.55	0.93
		SUN	0.36	0.82	0.61	0.81
Teff	≥ median vs < median	NIVO+IPI	0.75	0.83	0.92	0.93
		SUN	0.59	0.82	0.41	0.81
Myeloid	≥ median vs < median	NIVO+IPI	0.30	0.82	0.93	0.93
		SUN	0.85	0.98	0.75	0.81
Combined Myeloid and Teff	Myeloid score ≥ median vs < median	NIVO+IPI (patients with Teff score ≥ median)	0.26	0.82	0.42	0.93
		SUN (patients with Teff score ≥ median)	0.43	0.82	0.33	0.81
Combined Teff and Angio	Teff score ≥ median vs < median	NIVO+IPI (patients with Angio score < median)	0.83	0.83	0.18	0.93
		SUN (patients with Angio score < median)	0.54	0.82	0.81	0.81

^aNominal and adjusted p values are shown to accompany figure 3. Adjusted p values were corrected for multiple hypothesis testing using the Benjamini–Hochberg procedure. Angio, angiogenesis; IPI, ipilimumab; NIVO, nivolumab; OS, overall survival; PFS, progression-free survival; SUN, sunitinib; Teff, T-effector; TIS, tumor inflammation signature.

Supplementary methods

Trial design

CheckMate 214 (NCT02231749) was a randomized, phase 3 trial in adults with previously untreated, histologically advanced RCC with a clear-cell component.¹ Eligibility criteria (previously reported) included measurable disease according to Response Evaluation Criteria in Solid Tumors (RECIST) v1.1² and a Karnofsky performance status score of at least 70 (on a scale from 0 to 100, with lower scores indicating greater disability).¹ This trial was approved by the institutional review board or ethics committee at each site and was conducted according to Good Clinical Practice guidelines, defined by the International Conference on Harmonisation.¹ All the patients provided written informed consent that was based on the Declaration of Helsinki principles.¹

Assessment of clinical response

Response outcomes were confirmed and reported per independent radiology review committee using RECIST v1.1; best overall response was also assessed per investigator.³ Patients with complete response and partial response were classified as responders; patients with stable disease, progressive disease, and those who were non-evaluable were classified as non-responders. Objective response rate was defined as the number of responders divided by the total number of patients. PFS and OS were defined as the time from treatment initiation to documented evidence of progressive disease or death, respectively.

Whole-exome sequencing (WES)

DNA was extracted from tumor samples and blood samples using the Qiagen DNA FFPE and Qiagen DNA Blood Mini Kit, respectively (Qiagen, Germantown, CA). Whole-exome libraries for tumor and blood DNA samples were prepared using the SureSelectXT v5 Kit (Agilent) following validated standard operating procedures for DNA extracted from tumors and germline control samples. Briefly, extracted DNA was fragmented using sonication with a Covaris instrument (Covaris, Woburn, MA). Whole-genome libraries were prepared and subjected to a liquid-phase hybridization capture step that aimed to enrich for exonic regions of protein-coding genes. Enrichment of libraries and addition of a sample barcode index was achieved using a post-capture polymerase chain reaction (PCR) step. Libraries were then quantitatively and qualitatively evaluated using quantitative PCR (qPCR) and a D1000 Assay using TapeStation (Agilent), respectively. Finally, equimolar amounts of libraries were pooled and sequenced using the Illumina HiSeq2500 (Illumina, San Diego, CA) following 2×100 paired-end sequencing, targeting a depth of coverage of 100 \times . Sequence alignment and variant calling were performed using a published WES processing pipeline based on Human Build 37 (GRCh37).⁴

Mutation status

Patients were categorized as MUT if truncating (nonsense, nonstop, frameshift deletion/insertion, splice site), missense mutations, or inframe deletions/insertions were present, or WT if no such mutations were present. Genes that were mutated in ≥10 patients were included in the analysis. For each gene, two Cox proportional-hazards models were used to select those genes where mutation status was significantly associated with OS (nominal P value without multiple hypothesis correction <0.05): (i) patients from both treatment arms, including an interaction term of mutation status and treatment arm; (ii) patients in the nivolumab plus ipilimumab arm only. Analyses were then adjusted for multiple hypothesis testing using the Benjamini-Hochberg Procedure.⁵ Additional genes were included for further analysis based on previously reported associations in RCC.⁶⁻⁸ Volcano plots were generated using R v3.6.1 (2019-07-05). OncoPrint was used to visualize the frequency of mutations in selected genes and was generated using a local installation of cBioPortal (v3.4.12).⁹

RNA sequencing (RNA-seq)

Whole-transcriptome RNA-seq libraries were prepared using TruSeq Stranded Total RNA Kit with Ribo-Zero (Illumina) following a validated standard operating procedure. Briefly, total RNA samples were normalized for concentration before undergoing ribosomal RNA (rRNA) depletion using biotin-labeled probes. rRNA-depleted RNA was fragmented using heat in the presence of divalent cations. Fragments were randomly primed for first- and second-strand complementary DNA (cDNA) synthesis. Double-stranded

cDNA underwent end-repair, A-tailing, and ligation of adapters that included index sequences. Library constructs were subsequently amplified using PCR. Libraries were then quantitatively and qualitatively evaluated using qPCR and a D1000 Assay using TapeStation (Agilent), respectively. Finally, equimolar amounts of libraries were pooled and sequenced using NovoSeq (Illumina) following 2 × 100 paired-end sequencing, targeting a depth of 80 million reads.

RNA-seq quality control and processing

Raw RNA-seq reads were aligned and filtered using STAR v2.6.0c.¹⁰ After removing microbial contaminants, sequences were aligned to the human reference genome GRCh38 using the Ensembl 91 gene model, and read counts were quantified using RSEM. Sequencing quality was assessed using the Picard QC tool kit (v1.14; <http://broadinstitute.github.io/picard/>) and DupRadar (<https://bioconductor.org/packages/release/bioc/html/dupRadar.html>)¹¹ to ensure adequate transcriptome coverage and quantify PCR artifacts. Samples with Picard MarkDuplicates Estimated Library Size <2 million or DupRadar Deduplicated Dynamic Range <265 were excluded. Quantified raw counts from the remaining samples were normalized using edgeR's trimmed mean of M values method,¹² and normalized counts per million were log2-transformed for further analysis.

Tumor microenvironment deconvolution using MCP-counter

A transcriptome-based cellular deconvolution method called MCP-counter (<https://github.com/ebecht/MCPcounter>)¹³ was applied to RNA-seq samples to estimate the abundance of eight tumor-infiltrating IC populations (CD3+ T cells, CD8+ T cells, cytotoxic lymphocytes, natural killer cells, B lymphocytes, monocytic lineage cells, myeloid dendritic cells, and neutrophils) and two stromal cell populations (endothelial cells and fibroblasts) within the tumor microenvironment. Association analysis was performed on the abundance scores of the ten cell types with PFS and OS within each arm. P values were adjusted using Benjamini–Hochberg correction for multiple hypothesis testing.⁵ Unsupervised hierarchical clustering was also performed (using ward.D2) to group RNA-seq–evaluable patients into five clusters based on cell abundance scores. Principle Component Analysis (PCA) was also performed to visualize the five clusters using the first two PCs. Correlation of each cell type with each PC was performed to determine the major cell type contributors to each PC.

Supplementary references

1. Motzer RJ, Tannir NM, McDermott DF, et al. Nivolumab plus ipilimumab versus sunitinib in advanced renal-cell carcinoma. *N Engl J Med* 2018;378:1277–90.
2. Eisenhauer EA, Therasse P, Bogaerts J, et al. New response evaluation criteria in solid tumours: revised RECIST guideline (version 1.1). *Eur J Cancer* 2009;45:228–47.

3. Motzer RJ, Escudier B, McDermott DF, et al. Survival outcomes and independent response assessment with nivolumab plus ipilimumab versus sunitinib in patients with advanced renal cell carcinoma: 42-month follow-up of a randomized phase 3 clinical trial. *J Immunother Cancer* 2020;8:e000891.
4. Chang H, Sasson A, Srinivasan S, et al. Bioinformatic methods and bridging of assay results for reliable tumor mutational burden assessment in non-small cell lung cancer. *Mol Diagn Ther* 2019;23:507–20.
5. Benjamini Y, Hochberg Y. Controlling the false discovery rate: a practical and powerful approach to multiple testing. *J R Statist Soc B* 1995;57:289–300.
6. Motzer RJ, Robbins PB, Powles T, et al. Avelumab plus axitinib versus sunitinib in advanced renal cell carcinoma: biomarker analysis of the phase 3 JAVELIN Renal 101 trial. *Nat Med* 2020;26:1733–41.
7. Braun DA, Hou Y, Bakouny Z, et al. Interplay of somatic alterations and immune infiltration modulates response to PD-1 blockade in advanced clear cell renal cell carcinoma. *Nat Med* 2020;26:909–18.
8. McDermott DF, Huseni MA, Atkins MB, et al. Clinical activity and molecular correlates of response to atezolizumab alone or in combination with bevacizumab versus sunitinib in renal cell carcinoma. *Nat Med* 2018;24:749–57.
9. Gao J, Aksoy BA, Dogrusoz U, et al. Integrative analysis of complex cancer genomics and clinical profiles using the cBioPortal. *Sci Signal* 2013;6:pl1.
10. Dobin A, Davis CA, Schlesinger F, et al. STAR: ultrafast universal RNA-seq aligner. *Bioinformatics* 2013;29:15–21.
11. Sayols S, Scherzinger D, Klein H. dupRadar: a Bioconductor package for the assessment of PCR artifacts in RNA-Seq data. *BMC Bioinformatics* 2016;17:428.
12. Robinson MD, Oshlack A. A scaling normalization method for differential expression analysis of RNA-seq data. *Genome Biol* 2010;11:R25.
13. Becht E, Giraldo NA, Lacroix L, et al. Estimating the population abundance of tissue-infiltrating immune and stromal cell populations using gene expression. *Genome Biol* 2016;17:218.